Experimental Water and Air Cooling Performance of a Solar Powered Thermoelectric Module Across a Battery Discharge Cycle

T. Haritha[1*]; M. T. Naik[2]

[1]M.Tech Scholar; [2]Senior Professor

[1,2]Centre for Energy Studies, Department of Mechanical Engineering JNTUH College of Engineering (Autonomous), Jawaharlal Nehru Technological University Hyderabad 500085, Telangana, India

Corresponding Author: T. Haritha[1*]

Publication Date: 2026/09/04

Abstract: This paper reports the design, fabrication and experimental evaluation of a stand alone solar powered thermoelectric cooling unit that chills both water and air, and characterises it through a complete battery discharge cycle, the module being supplied directly from the battery without voltage regulation on the load side. The unit uses a single TEC1 12706 bismuth telluride module supplied from a 12 V, 8 Ah sealed lead acid battery that is charged by a 20 W polycrystalline photovoltaic panel through a 12 V, 5 A charge controller. Waste heat at the hot junction is rejected by an aluminium finned heat sink and a direct current fan, while the cold junction is coupled either to an insulated vessel of water or to a finned radiator placed inside a rectangular duct of cross section 22 cm by 5 cm by 2.5 cm. In the water cooling mode the load was brought from 23.5 degree Celsius to 2.1 degree Celsius in 139 minutes, a reduction of 21.4 kelvin, while the hot face settled near 39 degree Celsius. In the air cooling mode seven runs at different states of battery charge produced outlet air temperature reductions between 3.4 and 12.3 kelvin, with a mean reduction of 7.3 kelvin, accompanied by a mean loss of about 51 percent in air velocity caused by the flow resistance of the finned radiator, a trade off the duct was built to quantify. For a 250 millilitre load the mean cooling capacity was 2.69 watts over the whole run and 6.70 watts over the initial linear regime, giving a peak coefficient of performance of about 0.11. The results show that the cooling rate is governed mainly by the supply voltage and by the effectiveness of hot side heat rejection, and that the cold face temperature falls asymptotically as the temperature difference across the module approaches its limiting value. The system needs no refrigerant, has no moving part other than the fans, and responds within seconds of switching, which suits it to small capacity point of use cooling and heating, to laboratory and research duty requiring a controlled surface temperature, and to service in locations where grid electricity is unreliable.

Keywords: *Thermoelectric Cooling; Peltier Effect; Photovoltaic; Solar Refrigeration; TEC1 12706; Coefficient of Performance.*

Nomenclature: *α Seebeck coefficient of the couple (V/K) ; I electric current (A); R electrical resistance of the module (Ω); K thermal conductance of the module (W/K); Tc cold face temperature (K or °C); Th hot face temperature (K or °C); ΔT temperature difference across the module (K); Qc cooling capacity (W); P electrical power input (W); COP coefficient of performance; ZT dimensionless thermoelectric figure of merit; m mass of water (kg); cp specific heat capacity of water (J/kg K); TEC thermoelectric cooler; PV photovoltaic.*

How to Cite: T. Haritha; M. T. Naik. (2026) Experimental Water and Air Cooling Performance of a Solar Powered Thermoelectric Module Across a Battery Discharge Cycle. *International Journal of Innovative Science and Research Technology*, 11(8), 2714-2721. https://doi.org/10.38124/ijisrt/26aug1117

I. INTRODUCTION

Cooling is one of the fastest growing loads on the world electricity system. Air conditioners and electric fans already account for close to one fifth of the electricity used in buildings worldwide, energy use for space cooling has more than tripled since 1990, and in the absence of strong efficiency policy the demand is projected to more than double again by 2050 [1]. More than four fifths of that growth is expected in emerging and developing economies, and in India alone the share of space cooling in peak electrical load may rise from about a tenth today to nearly half by 2050 [1], [2]. At the same time

ISSN No:-2456-2165 https://doi.org/10.38124/ijisrt/26aug1117

roughly three and a half billion people live in hot regions where only about one household in seven owns a cooling appliance, so the demand is not merely a matter of comfort but of health, food security and labour productivity [2].

This growth is occurring under a tightening regulatory constraint. The Kigali Amendment to the Montreal Protocol, in force since 2019, commits its parties to a phased reduction of hydrofluorocarbon refrigerants whose global warming potential is hundreds to thousands of times that of carbon dioxide [3]. Vapour compression remains by far the most efficient way to move large quantities of heat, but for small, distributed or intermittently used loads the combination of a charged refrigerant circuit, a rotating compressor and a dependable alternating current supply is increasingly awkward. Solid state cooling, which needs none of the three, has therefore returned to attention.

The physical basis is old. Seebeck observed in 1821 that a current flows in a closed circuit of two dissimilar conductors whose junctions are held at different temperatures. Peltier found in 1834 that the converse holds, and Lenz showed in 1838 that a current driven through such a junction could freeze water at one end or melt ice at the other according to its direction. Altenkirch established in the early twentieth century that a useful thermoelectric material must combine a large Seebeck coefficient with high electrical and low thermal conductivity, a requirement later expressed as the dimensionless figure of merit ZT. The field became practical only when Ioffe showed in the 1950s that doped semiconductors, rather than metals, could satisfy that combination [4], and bismuth telluride alloys have remained the working material of commercial Peltier modules ever since.

Progress since then has been steady rather than dramatic, but it has not stopped. Commercial modules have long operated near a peak ZT of about one, and the consensus is that ZT would need to approach two before thermoelectric cooling could challenge vapour compression on efficiency. Recent materials work has narrowed that gap: compositional and defect engineering of $(Bi,Sb)_2Te_3$ has produced a peak ZT of about 1.50 near 348 K together with a substantial gain in mechanical strength, and micro coolers built from that material have reached a maximum temperature difference of 89.3 K [5], [6]. Nanocomposite routes, in which second phase inclusions scatter phonons more strongly than charge carriers, are being pursued along the same lines [7]. These advances have so far been demonstrated chiefly at the material and micro device scale; the modules available to a designer of a small appliance, including the TEC1 12706 used here, still perform close to their long established catalogue values, which is why device level thermal design remains the dominant factor in practice.

The second change since the technology was last widely assessed is on the supply side. The installed cost of photovoltaic generation has fallen by roughly an order of magnitude over the past fifteen years, which alters the economic comparison for any small cooling duty that can be met directly from a panel and a battery. Recent experimental work reflects this: photovoltaic thermoelectric units have been shown to hold vaccines within the 2 to 8 °C band required for cold chain storage, with autonomy of several hours from battery support [8], and phase change material has been integrated into the cold side of solar thermoelectric refrigerators to extend that autonomy across periods without irradiance [9]. The application space for thermoelectric cooling is thus better defined than it once was. It is not a competitor to domestic or commercial air conditioning; it is a candidate wherever the load is small, the duty is intermittent, the supply is unreliable, and silence, compactness, orientation independence or freedom from refrigerant carries weight.

Configurations of this kind have been reported before, and the present contribution should be read against them. Solar driven TEC1-12706 units bonded to an insulated water vessel with a finned heat sink and fan on the hot face have been built and instrumented, most recently with networked monitoring added [10]; cooler box studies with the same module have established that the coefficient of performance falls as the run proceeds and have optimised module placement [11]; multi stage solar Peltier water coolers have been examined both experimentally and by computational fluid dynamics [12]; and a solar thermoelectric air conditioning system tested in Baghdad reported that the inlet air velocity directly influences both the coefficient of performance and the outlet air temperature [13]. What has not been reported together, so far as the authors are aware, are three things that this paper supplies: a direct comparison of water and air duty using one module and one power train, so that the two are measured under identical hardware; the transient behaviour of both module faces through a complete battery discharge cycle, which is the condition an off grid unit actually experiences and which reveals the convergence of the two faces as the supply collapses; and a quantified measurement of the velocity penalty imposed by the cold side radiator, a cost that is acknowledged qualitatively in the literature but seldom given a number. These are incremental contributions to a well populated field rather than a new principle, and they are offered as such.

The present work sits in that space. A single commercial module was coupled to a photovoltaic source and a battery, and its transient behaviour was measured in two distinct duties: chilling a static body of water, and chilling a forced air stream passing through a duct. The objectives were to build and instrument a working prototype, to record both faces of the module through a complete discharge so that the influence of a falling, falling supply voltage could be observed, to quantify the reduction in temperature and the accompanying loss of velocity in the air stream, and to identify which of the several possible constraints actually limits performance in a unit of this class.

II. LITERATURE REVIEW

Abdullah and co workers studied a combined solar thermoelectric and adsorption cooling system over eight days. Cooling was produced thermoelectrically during the day and by the adsorption cycle at night; the coefficient of performance was 0.152 for the thermoelectric part and 0.131 for the adsorption part [15].

Luo reported that heating produced by a thermoelectric device was moderately more efficient than direct resistance

ISSN No:-2456-2165 https://doi.org/10.38124/ijisrt/26aug1117

heating [16]. Gillott and co workers tested thermoelectric modules for space conditioning inside buildings and obtained 220 W of cooling from eight ultra thermoelectric units at a current of 4.9 A per module, with a coefficient of performance of 0.48 [17].

Riffat and Qiu compared a thermoelectric air conditioning system with vapour compression and vapour absorption machines and found the thermoelectric coefficient of performance to be appreciably lower [18]. Bansal and Martin compared three domestic refrigerators of similar capacity and reported coefficients of performance of 2.57 for vapour compression, 0.68 for the thermoelectric unit and 0.46 for the absorption unit, while noting that the thermoelectric technology is mature, reliable and inexpensive [19].

Min and Rowe built several prototype thermoelectric coolers and compared them on coefficient of performance, temperature stability, heat pumping capacity and rate of cooling; for a cabinet at 5 °C in an ambient of 25 °C the coefficient of performance lay between 0.3 and 0.5, and they concluded that improving the thermal interfaces is the most effective route to better performance [20].

Chen and co workers analysed single stage and two stage arrangements using non equilibrium thermodynamics and showed that the choice between them depends on the ratio of sink temperature to cooled space temperature: for a small ratio the single stage device is preferable, for a large ratio the two stage device gives both a higher coefficient of performance and a higher rate of refrigeration [21]. Xuan examined two stage coolers in pyramid and cuboid configurations and found the optimum ratio of module numbers, or of stage currents, to lie between 2.5 and 3 [22]. Luo and co workers applied finite time thermodynamics and showed that the total heat transfer surface area of the exchangers and the operating current dominate the optimum cooling load and coefficient of performance [23]. Dhawade reviewed portable solar thermoelectric refrigerators and emphasised their suitability for rural areas with an unreliable supply [24].

Alongside these, thermoelectric cold chain chests [14], solar driven water condensation using the Peltier effect [25], cascaded Peltier arrangements [26], Peltier based room air conditioners [27] and portable solar refrigeration units [28] indicate the breadth of the application space. Taken with the photovoltaic work cited in Section I [8], [9], the reviewed literature establishes the performance envelope of thermoelectric cooling but reports comparatively little transient data for a directly photovoltaic powered unit operating on a falling battery voltage, and little on the penalty that a cold side radiator imposes on the air stream. Those two gaps motivate the present measurements.

III. SYSTEM DESCRIPTION AND EXPERIMENTAL METHOD

➢ *Layout of the System*

Fig 1 shows the arrangement. A 20 W photovoltaic panel charges the battery through a charge controller; the battery supplies the Peltier module and the fan. The hot face of the module is bonded to an aluminium heat sink cooled by a direct current fan, and the cold face is bonded either to the base of an insulated stainless steel vessel holding water or to a finned radiator mounted inside a rectangular duct.

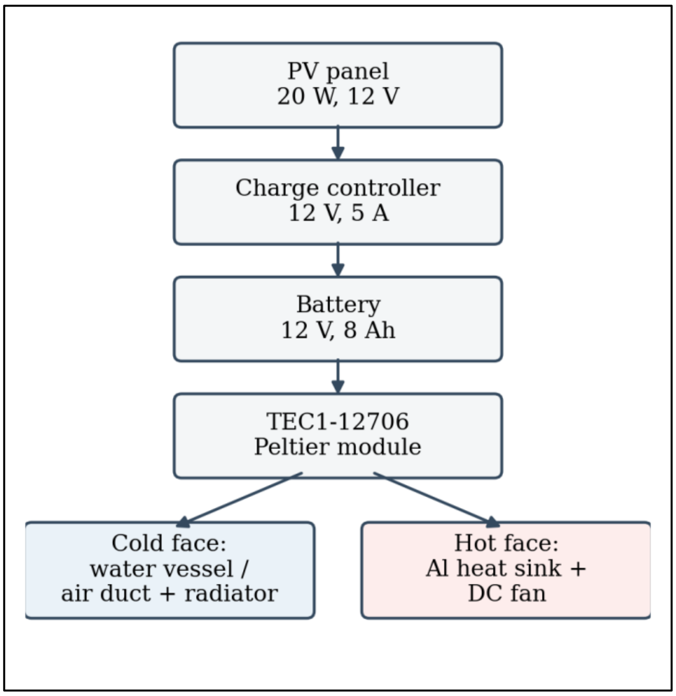

Fig 1 Block Diagram of the Solar Powered Thermoelectric Cooling Unit

➢ *Components*

- Photovoltaic panel: polycrystalline, 20 W peak, 16.4 V at maximum power, 1.22 A at maximum power, open circuit voltage 21.0 V, short circuit current 1.60 A, rated at 1000 W per square metre and 25 °C.
- Charge controller: 12 V, 5 A, providing protection against overcharge, deep discharge and reverse current.
- Battery: sealed lead acid, 12 V, 8 Ah, charged for two full days before each test series. The charge controller regulates the charging side only; during a test the module and fan are supplied directly from the battery, so the voltage at the module falls as the battery discharges.
- Thermoelectric module: TEC1 12706, 40 mm by 40 mm by 3.8 mm, 127 couples, maximum current 6.4 A, maximum voltage 14.4 V at a hot side of 25 °C.
- Heat rejection: extruded aluminium finned heat sink with thermal paste at the interface and a 12 V direct current fan.
- Instruments: two digital contact temperature sensors with a resolution of 0.1 K, a hot wire digital anemometer covering 0 to 30 metres per second and minus 10 to 45 °C, and a digital multimeter.

ISSN No:-2456-2165 https://doi.org/10.38124/ijisrt/26aug1117

Table 1 Manufacturer Performance Data for the TEC1 12706 Module

Parameter	**Th = 25 °C**	**Th = 50 °C**
Qmax (W)	50	57
Delta Tmax (K)	66	75
Imax (A)	6.4	6.4
Vmax (V)	14.4	16.4
Resistance (ohm)	1.98	2.30

- *Test Procedure*

Two independent sets of measurements were made. In the water cooling test the vessel was filled, the sensors were placed in the water and on the hot face, the module was energised from the fully charged battery and both temperatures were logged at intervals until the water temperature became stationary. In the air cooling test a blower delivered air to the duct, the inlet and outlet air temperature and velocity were measured with the anemometer, and the two faces of the module and the battery terminal voltage were recorded simultaneously. The duct was deliberately built as a simple rectangular section so that the entering stream was forced through the radiator fins rather than around them. Measuring the velocity on both sides of the fin block was an explicit objective rather than an incidental observation: the same extended surface that transfers heat to the air also obstructs it, and the resulting loss of mass flow offsets part of the temperature reduction gained. Quantifying that trade off requires velocity to be measured at inlet and outlet under the same conditions as temperature. The runs were repeated at successively lower states of charge so that the influence of supply voltage could be separated. A recovery interval of at least four hours was allowed between runs. Ambient temperature during the charging test was 30 plus or minus 0.5 °C. Throughout this paper absolute temperatures are reported in degrees Celsius (°C) and temperature differences in kelvin (K), the numerical value of an interval being identical in the two units.

IV. THERMODYNAMIC ANALYSIS

The heat absorbed at the cold junction by the Peltier effect is the product of the Seebeck coefficient, the current and the cold junction temperature. Against this useful effect act one half of the Joule heat generated in the pellets, which divides equally between the two faces, and the heat conducted back from the hot face through the pellets. The net cooling capacity is therefore

$$Q_c = \alpha I T_c - 0.5 I^2 R - K (T_h - T_c) \quad (1)$$

where alpha is the Seebeck coefficient of the couple, I the current, R the electrical resistance of the module, K its thermal conductance, and Tc and Th the absolute temperatures of the cold and hot faces. The electrical power drawn by the module is

$$P = \alpha I (T_h - T_c) + I^2 R \quad (2)$$

the first term representing the work done against the Seebeck voltage that the temperature difference itself generates, and the second the ohmic loss. The coefficient of performance follows as

$$COP = Q_c / P \quad (3)$$

Equations (1) and (2) explain the two limits observed in the experiment. As the temperature difference grows, the conduction term in (1) grows with it while the Peltier term does not, so the net cooling capacity falls towards zero at the limiting temperature difference; at the same time the first term of (2) grows, so the power drawn rises and the coefficient of performance falls. Effective hot side heat rejection, which keeps Th low, therefore improves both the capacity and the efficiency.

- *Energy Balance of the Prototype*

With the module and fan drawing about 6 A at 12 V the connected load is 72 W. The stored energy of the 12 V, 8 Ah battery is 96 Wh, which gives a theoretical run time of 1.33 h at that load. The measured run time was 1 h 35 min, from which the mean draw over the discharge is 60.6 W rather than 72 W. The difference is consistent with the fall of terminal voltage during discharge and the reduction of module current that accompanies it, and it is the reason the nominal load overstates the input power in the efficiency figures that follow. Recharging 96 Wh from a 20 W panel requires about 4.8 h of full irradiance, and correspondingly longer under the varying irradiance of a real day, which is why two days of charging were allowed before the test series.

V. RESULTS AND DISCUSSION

- *Charging Behaviour*

Figure 2 shows the terminal voltage of the battery during charging from the panel on a clear day. The voltage rose steadily from 10.1 V to 13.0 V over eight hours, an almost linear rise of about 0.36 V per hour, indicating that the panel was operating well below the current at which the controller would begin to limit.

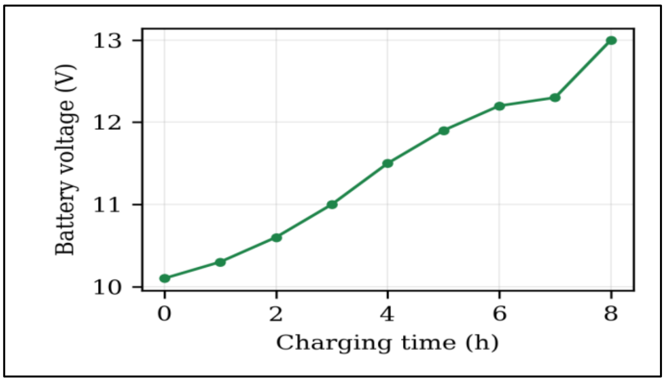

Fig 2 Battery Terminal Voltage During Charging from the 20 W Panel

ISSN No:-2456-2165 https://doi.org/10.38124/ijisrt/26aug1117

➢ *Water Cooling*

Table 2 lists the water temperature and the hot face temperature. The water fell from 23.5 °C to 2.1 °C in 139 minutes, a reduction of 21.4 K, without reaching the freezing point.

Table 2 Transient Temperatures During the Water Cooling Test

Time (min)	**Tc (°C)**	**Th (°C)**
0	23.5	28.0
2	22.0	48.4
6	20.0	43.4
12	17.8	38.3
19	15.7	37.2
25	13.9	37.0
34	12.0	39.7
43	10.0	41.2
55	8.0	40.8
78	5.8	40.5
106	4.0	39.8
139	2.1	38.9

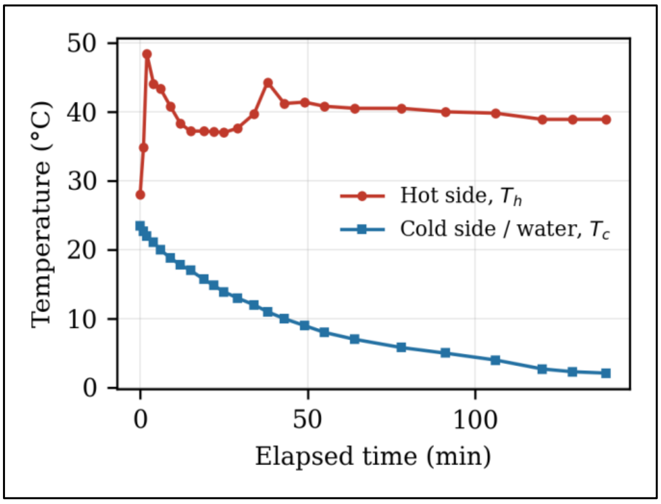

Fig 3 Cold Face and Hot Face Temperature Against Time

The curves in Fig 3 show three distinct regimes. In the first two minutes the hot face rose sharply from 28.0 to 48.4 °C because the heat sink and fan had not yet reached their steady state, while the water had barely begun to respond. Between about 5 and 30 minutes the hot face settled near 37 °C and the water fell almost linearly at 0.38 K/min, the interval of greatest cooling capacity. Beyond about 90 minutes the rate fell to 0.06 K/min as the temperature difference across the module approached its limit and the conduction term of (1) consumed an increasing share of the Peltier cooling.

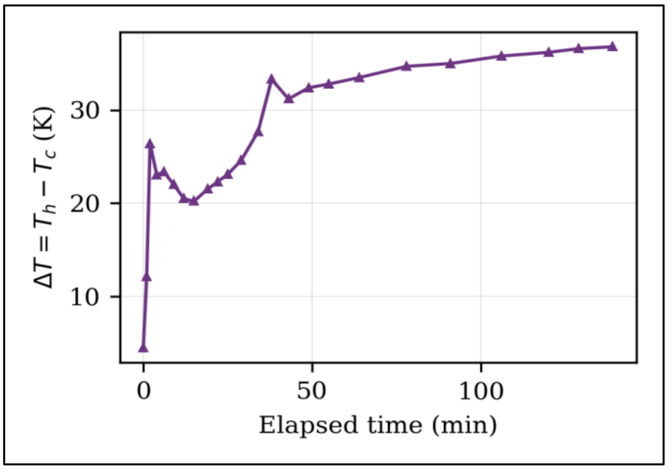

Fig 4 Temperature Difference Across the Module Against Time

Fig 4 confirms this reading. The temperature difference across the module grew from 4.5 K at the start to about 36.8 K at the end of the run, roughly 56 percent of the 66 K quoted by the manufacturer for a hot side of 25 °C. The shortfall is attributable to the hot face running near 39 °C rather than 25 °C, to the thermal resistance of the vessel wall between the module and the water, and to heat gain from the surroundings through the walls of the vessel.

➢ *Cooling Capacity and Coefficient of Performance*

The vessel held 250 ml of water. Taking the specific heat capacity of water as 4186 J/kg K, the sensible heat removed over the run is m cp (Tc,initial minus Tc,final), which for a reduction of 21.4 K gives 22.4 kJ. Spread over the 139 minute run this corresponds to a mean cooling capacity of 2.69 W. The instantaneous capacity varies greatly across the run, however, and the mean understates what the module can do. Over the linear regime from 0 to 25 minutes the water fell 9.6 K, giving 6.70 W, whereas over the final 48 minutes it fell only 1.9 K, giving 1.05 W.

ISSN No:-2456-2165 https://doi.org/10.38124/ijisrt/26aug1117

Table 4 Cooling Capacity and Coefficient of Performance

Interval	Qc (W)	COP at 72 W	COP at 60.6 W
0 to 25 min (linear)	6.70	0.093	0.111
Whole run, 0 to 139 min	2.69	0.037	0.044
91 to 139 min (tail)	1.05	0.015	0.017

Two input powers are shown because the nominal connected load of 72 W overstates the power actually drawn as the battery voltage falls; 60.6 W is the mean derived in Section IV from the measured run time. The peak coefficient of performance of about 0.11 is low against the 0.3 to 0.5 reported for thermoelectric domestic refrigerators [20] but consistent with the 0.04 obtained for a multi stage solar Peltier water cooler [12]. Three factors account for the difference. The figure includes the fan power, which several published values exclude. It counts only the sensible heat of the water, ignoring the thermal mass of the vessel and the heat gained through its walls, so the true capacity is somewhat higher than stated. And the hot face ran near 39 °C rather than the 25 °C of the catalogue condition, which by (1) and (2) both reduces Qc and raises P. The figures should therefore be read as a conservative lower bound on the performance of the arrangement rather than as a material property.

➢ *Air Cooling*

Table 3 gives the seven air cooling runs, arranged in the order in which they were taken as the battery discharged.

Table 3 Air Cooling Test Results

Run	V (V)	Tc (°C)	Th (°C)	Vin (m/s)	Tin (°C)	Vout (m/s)	Tout (°C)
1	13.79	28.8	28.3	4.8	45.4	2.0	36.1
2	12.20	20.9	38.0	4.9	48.6	1.3	36.8
3	12.26	18.3	44.2	4.4	50.0	2.0	37.7
4	12.12	18.7	54.1	4.1	49.6	1.8	43.0
5	12.02	19.4	47.2	1.2	42.0	0.8	38.6
6	11.67	15.0	37.7	2.1	36.9	1.2	33.2
7	6.70	12.0	34.0	3.2	37.3	2.0	33.4

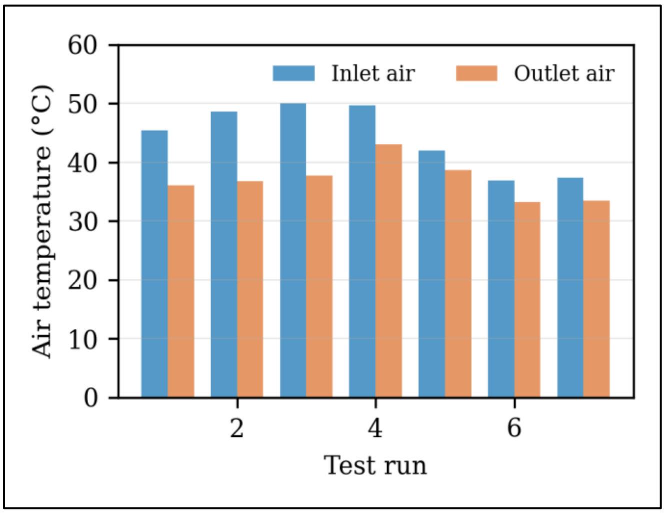

Fig 5 Inlet and Outlet Air Temperature for Each Run

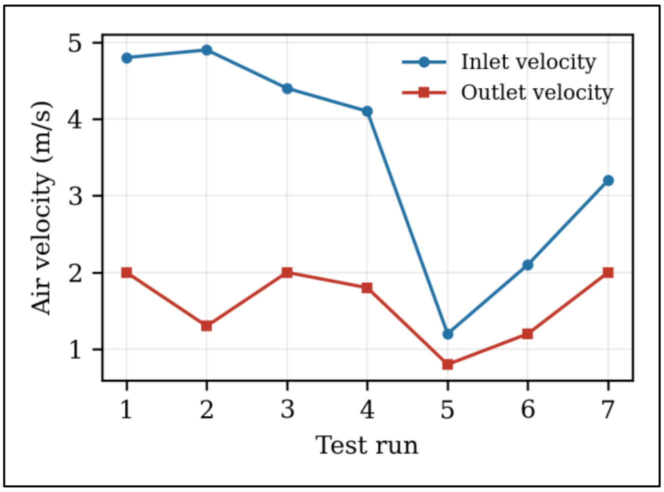

Fig 6 Inlet and Outlet Air Velocity for Each Run

The reduction in air temperature ranged from 3.4 to 12.3 K with a mean of 7.3 K. The largest reductions occurred in runs 2 and 3, where the inlet air was hottest and the module was still supplied at more than 12 V; the smallest occurred in runs 5 to 7, where either the inlet air was already close to the cold face temperature or the supply had collapsed. Run 4 is instructive: the hot face reached 54.1 °C, the highest recorded, and the temperature reduction fell to 6.6 K even though the supply voltage was almost unchanged, which demonstrates directly that inadequate hot side rejection, rather than the supply, was limiting at that point.

Fig 6 shows the hydraulic penalty. The finned radiator reduced the air velocity by between 33 and 74 percent, with a mean of about 51 percent. This is a real limitation of the arrangement: the fins that are needed to transfer heat to the air also obstruct it, and because the mass flow falls the total cooling delivered to the space falls with it even when the temperature reduction per unit mass is favourable.

ISSN No:-2456-2165 https://doi.org/10.38124/ijisrt/26aug1117

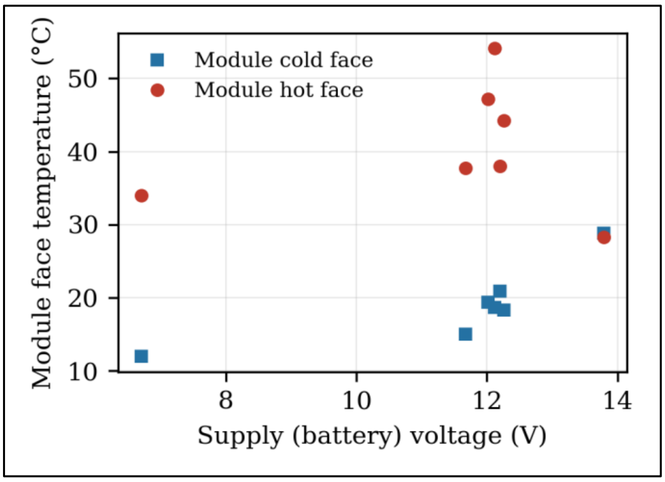

Fig 7 Module Face Temperatures Against Supply Voltage

Fig 7 collects the module face temperatures against the battery voltage. The cold face temperature is lowest at the lowest voltage while the hot face is also lowest there, so the two faces converge as the supply falls: at 6.70 V the difference across the module is only 22 K against 35.4 K at 12.12 V. Because the cooling capacity depends on the current and not on the face temperature alone, a low cold face temperature reached at a collapsed supply does not correspond to useful cooling. This is the practical reason for the charge controller and for the recommendation that the battery be kept above its nominal voltage during operation.

➢ *Application Space of the Unit*

The measured behaviour indicates where a unit of this class is useful. It is not a substitute for domestic refrigeration or for space air conditioning, whose loads are one to two orders of magnitude larger. Its value lies in three kinds of duty.

- Laboratory and research use. Because the cold face responds within seconds of switching and its temperature can be set by adjusting the supply current, the module is a convenient bench source of a controlled low temperature for calibrating sensors, conditioning small samples, holding reagents, stabilising optoelectronic components such as laser diodes and image sensors, and providing a cold surface for condensation or dew point work. Commercial temperature controllers hold a set point to within about 0.5 K, which is closer than a cycling compressor can manage.
- Rapid, intermittent point of use cooling. The prototype removed heat at its greatest rate during the first thirty minutes of operation, at 0.38 K/min, before the temperature difference across the module approached its limit. Duties that need a moderate temperature reduction quickly and then stop, such as chilling a single beverage, a small sample container or a personal air stream, exploit exactly that part of the characteristic and avoid the inefficient tail.
- Heating and thermal cycling. Reversing the polarity of the supply exchanges the two faces, so the same hardware serves as a compact heater or as a means of cycling a specimen between a warm and a cold state without any change of equipment. In the present tests the hot face reached 54.1 °C against an ambient near 30 °C, which indicates the heating capability available from a single module. It should be noted that repeated polarity reversal stresses the solder joints within the module and shortens its life, so where continuous heating is required a resistance element bonded to the cold side heat sink is the better arrangement.

Common to all three is that the load is small, the duty is intermittent, and the qualities the module offers, namely fast response, close set point control, silence, freedom from refrigerant, tolerance of any mounting orientation and the ability to run directly from a low voltage direct current source, matter more than the coefficient of performance.

➢ *Limitations*

- The mass of water was not recorded, so the cooling load in watts and hence the experimental coefficient of performance could not be evaluated. Only the manufacturer data and the transient temperatures are available.
- The module current was not logged continuously, so the analysis of Section IV relies on the nominal load rather than measured input power.
- The air cooling runs were taken at different inlet conditions as well as at different supply voltages, so the two influences are not fully separated.
- Solar input is intermittent, and the panel area required grows quickly with cooling capacity, which restricts the technology to small loads.

VI. CONCLUSION

A photovoltaic powered thermoelectric unit was built and tested in both water cooling and air cooling modes. The unit reduced the temperature of a body of water by 21.4 K in a little over two hours and reduced the temperature of a forced air stream by a mean of 7.3 K, reaching a peak coefficient of performance of about 0.11 for a 250 millilitre load. The measurements show that performance is limited chiefly by the hot side heat rejection and by the supply voltage: the cooling rate is greatest while the hot face is held near 37 °C and falls sharply once it rises above 45 °C, and the temperature difference achieved across the module reached only about 56 percent of the manufacturer limiting value. The radiator that couples the cold face to the air stream halved the air velocity, so future work should address the hydraulic design of that element as well as the thermal design. Within these limits the unit provides refrigerant free, silent, orientation independent cooling with no moving part other than the fans, and is suited to small, point of use duty. Beyond off grid service in locations without a dependable supply, the combination of fast response, close set point control and reversibility of the temperature gradient makes the arrangement well suited to laboratory and research use and to rapid, intermittent cooling or heating of small loads.

ACKNOWLEDGMENT

The authors thank the Centre for Energy Studies, JNTUH College of Engineering Hyderabad, for the laboratory facilities used in this work, and Dr. K. V. Sharma for his advice during the experimental programme.

ISSN No:-2456-2165 https://doi.org/10.38124/ijisrt/26aug1117

REFERENCES

[1]. International Energy Agency, The Future of Cooling: Opportunities for Energy Efficient Air Conditioning. Paris: IEA, 2018.

[2]. International Energy Agency, "Staying cool without overheating the energy system," IEA Commentary, Paris, 2025.

[3]. United Nations Environment Programme, The Kigali Amendment to the Montreal Protocol on Substances that Deplete the Ozone Layer. Nairobi: UNEP, 2016.

[4]. A. F. Ioffe, Semiconductor Thermoelements and Thermoelectric Cooling. London: Infosearch Limited, 1957.

[5]. H.-L. Zhuang, B. Cai, Y. Pan, B. Su, Y. Jiang, J. Pei, F. Liu, H. Hu, J. Yu, J.-W. Li, Z. Wang, Z. Han, H. Li, C. Wang, and J.-F. Li, "Strong and efficient bismuth telluride-based thermoelectrics for Peltier microcoolers," National Science Review, vol. 11, no. 10, nwae329, 2024.

[6]. N. S. Chauhan and T. Mori, "Cooler, stronger, smaller: improving thermoelectric cooling," National Science Review, vol. 12, no. 1, nwae445, 2025.

[7]. H.-L. Zhuang, J. Yu, and J.-F. Li, "Nanocomposite strategy toward enhanced thermoelectric performance in bismuth telluride," Small Science, vol. 5, 2400284, 2025.

[8]. S. Uzair, M. Ahmad, and A. Waheed, "Photovoltaic thermoelectric cooling system for off-grid vaccine refrigerator: an experimental study," Transactions of the Canadian Society for Mechanical Engineering, 2023.

[9]. L. Fenton, D. Mathew, and R. Kandasamy, "Solar-powered thermoelectric refrigeration with integrated phase change material: an experimental approach to food storage," Journal of Energy Storage, vol. 79, 110247, 2024.

[10]. P. Chairat and S. Wongwises, "Peltier water cooling system with solar energy and IoT technology demonstration set," Energy Engineering, vol. 122, no. 11, 2025.

[11]. A. Mainil, N. Nasruddin, and M. Idrus Alhamid, "Experimental performances of a thermoelectric cooler box with thermoelectric position variations," Case Studies in Thermal Engineering, vol. 12, pp. 168-178, 2018.

[12]. M. Atmaca and A. Pektemir, "Development of an automatic solar-powered domestic water cooling system with multi-stage Peltier devices," Renewable Energy, vol. 130, pp. 51-60, 2019.

[13]. A. Al-Musawi and H. Hasan, "Experimental investigation of a solar-powered thermoelectric air conditioning system based on the Peltier effect," Nanotechnology Perceptions, pp. 268-278, 2024.

[14]. S. Chatterjee and K. G. Pandey, "Thermoelectric cold-chain chests for storing and transporting vaccines in remote regions," Applied Energy, vol. 76, no. 4, pp. 415-433, 2003.

[15]. M. Abdullah, S. Riffat, and G. Qiu, "Performance of a combined solar thermoelectric and adsorption cooling system," Applied Thermal Engineering, vol. 29, pp. 2242-2249, 2009.

[16]. J. Luo, "Performance of a thermoelectric heating system compared with electrical resistance heating," Journal of Electronic Materials, vol. 40, pp. 1064-1069, 2011.

[17]. M. Gillott, L. Jiang, and S. Riffat, "An investigation of thermoelectric cooling devices for small scale space conditioning applications in buildings," International Journal of Energy Research, vol. 34, pp. 776-786, 2010.

[18]. S. Riffat and G. Qiu, "Comparative investigation of thermoelectric air conditioners versus vapour compression and absorption air conditioners," Applied Thermal Engineering, vol. 24, pp. 1979-1993, 2004.

[19]. P. Bansal and A. Martin, "Comparative study of vapour compression, thermoelectric and absorption refrigerators," International Journal of Energy Research, vol. 24, pp. 93-107, 2000.

[20]. G. Min and D. M. Rowe, "Experimental evaluation of prototype thermoelectric domestic refrigerators," Applied Energy, vol. 83, pp. 133-152, 2006.

[21]. J. Chen, Y. Zhou, H. Wang, and J. T. Wang, "Comparison of the optimal performance of single stage and two stage thermoelectric refrigeration systems," Applied Energy, vol. 73, pp. 285-298, 2002.

[22]. X. C. Xuan, "Optimum design of a thermoelectric device," Semiconductor Science and Technology, vol. 17, pp. 114-119, 2002.

[23]. J. Luo, L. Chen, F. Sun, and C. Wu, "Optimum allocation of heat transfer surface area for cooling load and COP optimisation of a thermoelectric refrigerator," Energy Conversion and Management, vol. 44, pp. 3197-3206, 2003.

[24]. M. B. Dhawade, "A review on solar thermoelectric refrigeration and cooling applications," International Journal of Engineering Research and Technology, vol. 4, pp. 231-235, 2015.

[25]. R. M. Atta, "Solar water condensation using thermoelectric coolers," International Journal of Water Resources and Arid Environments, vol. 1, no. 2, pp. 142-145, 2011.

[26]. S. Haidar and I. Isaac, "Thermoelectric cooling using Peltier cells in cascade," in Proceedings of the Southeastern Symposium on System Theory, 2004.

[27]. A. Jose, "Air conditioner using Peltier module," in Proceedings of the International Conference on Circuits, Power and Computing Technologies, 2015.

[28]. A. Kumar G. B., "Design and implementation of a Peltier based solar powered portable refrigeration unit," in Proceedings of the International Conference on Energy, Communication, Data Analytics and Soft Computing, 2017.